



Nontargeted identification and predicted toxicity of new byproducts generated from UV treatment of water containing micropollutant 2-mercaptobenzothiazole



Ping Jiang^a, Junlang Qiu^a, Yanpeng Gao^{a,b,*}, Mihaela I. Stefan^c, Xing-Fang Li^{a,*}

^a Division of Analytical and Environmental Toxicology, Department of Laboratory Medicine and Pathology, Faculty of Medicine and Dentistry, University of Alberta Edmonton, AB, T6G 2G3, Canada

^b Guangdong Key Laboratory of Environmental Catalysis and Health Risk Control, Guangzhou Key Laboratory Environmental Catalysis and Pollution Control, School of Environmental Science and Engineering, Institute of Environmental Health and Pollution Control, Guangdong University of Technology, Guangzhou 510006, China

^c Trojan Technologies, 3020 Gore Road, London, ON, N5V 4T7, Canada

ARTICLE INFO

Article history:

Received 14 May 2020

Revised 14 October 2020

Accepted 19 October 2020

Available online 20 October 2020

Keywords:

Nontargeted analysis

Disinfection byproducts (DBPs)

Transformation product

Benzothiazole

Photochemical degradation

Computational toxicity

ABSTRACT

Comprehensive identification of byproducts including intermediate transformation products (TPs) of micropollutants in source water is challenging and paramount for assessment of drinking water quality and treatment technologies. Here, we have developed a nontargeted analysis strategy coupled with computational toxicity assessment to identify indistinguishable TPs including isomers with large differences in toxicity. The new strategy was applied to study the UV treatment of water containing micropollutant 2-mercaptobenzothiazole (2-MBT), and it enabled successful identification of a total of 22 organic TPs. Particularly, the structures of nine new TPs were identified for the first time; in addition, three isomers (P2, P3, and P4) were distinguished from the toxic contaminant 2-hydroxybenzothiazole (2-OH-BT). Computational assessments indicate that estrogenic activity of the three isomers (P2–P4) is higher than that of 2-OH-BT. Mass balance study shows that the 22 organic products accounted for 70% of the 2-MBT degraded, while 30% may degrade to inorganic products. Most TPs are resistant to UV photolysis. Computational toxicity assessment predicted the TPs to increase inhibition of human thyroperoxidase activity although they have lower aquatic toxicity compared to original 2-MBT. This study emphasizes the importance of monitoring the 2-MBT photodegradation products and the overall toxicity of finished water whose production included a UV light-based treatment process.

© 2020 Elsevier Ltd. All rights reserved.

1. Introduction

Micropollutants present in both source water and recycled water for potable reuse remain a health concern (Alsbäcker et al., 2016; Merle et al., 2020). During water disinfection processes, micropollutants can transform into a number of disinfection byproducts (DBPs) that may have higher persistence and/or toxicity than their parent compounds (Richardson and Kimura, 2017). Recent studies have shown that mixtures of different DBPs can produce additive effects of cytotoxicity, genotoxicity and/or other biological effects (Lau et al., 2020; Mestankova et al., 2016). Advanced engineering solutions are required to remove micropollutants and their byproducts (Bond et al., 2020). Therefore, it is insufficient to identify only parent micropollutants for controlling drinking water

quality. Instead, a rather comprehensive identification of the trace levels of transformation products (TPs) produced during the treatment of water containing micropollutants is advisable. Comprehensive identification of TPs is analytically challenging because of their trace levels and lack of standards and instrumental sensitivity.

Benzothiazoles, an important group of heterocyclic compounds, have multiple uses among which as fungicides in a variety of consumer products (e.g. tires and food) (Avagyan et al., 2014; He et al., 2011; Margenat et al., 2018) and as vulcanization accelerators in rubber manufacturing (Luongo et al., 2016; Reddy and Quinn, 1997). Due to their widespread use, benzothiazoles are listed as high production volume chemicals. Particularly, 2-mercaptobenzothiazole is most widely used in rubber plumbing components that are in contact with drinking water. The estimated annual production in the early 2000s exceeded 40,000 tons in Western Europe alone. Consequently, benzothiazoles have been widely detected at concentrations ranging from sub-ng/L

* Corresponding authors.

E-mail addresses: yanpeng@ualberta.ca (Y. Gao), xingfang.li@ualberta.ca (X.-F. Li).

to mg/L levels in tap water, groundwater, and surface waters (Liao et al., 2018; Seel and et al., 2012; Wang et al., 2016). For instance, the occurrence of 2-MBT was reported in the drinking water of Ahvaz city, in water samples collected from the Karun river (Esmaili et al., 2020) and the riverine runoff of the Pearl River Delta with average concentrations of 24.3–87.4 ng/L (Ni et al., 2008). Toxicity studies of benzothiazoles have shown potential adverse effects on aquatic organisms and human health (Avagyan et al., 2014; Fries, 2011; Rodríguez et al., 2004; Wang et al., 2016), including genotoxicity, cytotoxicity, carcinogenicity, as well as modulation of the thyroid hormone (Liao et al., 2018). The predicted no effect concentration (PNEC) and lowest observed effect concentration (LOEC) were reported as 0.82 µg/L and 78 µg/L, respectively (European Union (EU), 2008). Additionally, occupational exposure to 2-MBT is potentially associated with an increased risk of developing bladder cancer in workers (Sorahan, 2009; USEPA, 2016).

Current wastewater treatment processes such as UV disinfection, chlorination and ozonation either do not result in the efficient removal of micropollutants containing the benzothiazole structural entity (Liao et al., 2018) or can lead to byproducts preserving the benzothiazole ring such as 2-hydroxybenzothiazole and benzothiazole (BT) in the treated water (Fiehn et al., 1998). Existing studies indicate that benzothiazoles can transform to other products during water treatment, but comprehensive identification of their transformation products is still desirable. Understanding the formation of TPs during the water treatment and their impact on water quality as a whole is critical for ensuring safe water for people and the aquatic species.

UV light-based advanced oxidation processes (UV/AOPs) were widely implemented to remediate natural waters or recycled water from persistent micropollutants while achieving enhanced disinfection, for the purpose of potable water production (Stefan, 2018). Several studies have reported that UV-based AOPs are efficient at degrading benzothiazoles in water (Andreozzi et al., 2001; Habibi et al., 2001; Malouki et al., 2004; Redouane-Salah et al., 2018; Serdechnova et al., 2014; Zajčková and Párkányi, 2008). The photodegradation kinetics of several benzothiazoles were also reported (Bahnmüller et al., 2015; Serdechnova et al., 2014; Zajčková and Párkányi, 2008), but their transformation products largely remain unknown. For instance, previous studies reported that the photochemical degradation of 2-MBT mainly resulted in the formation of BT and 2-OH-BT, while up to 68% of products were unidentified primarily due to the inability of the employed methods to detect accurately low analyte concentrations (Brownlee et al., 1992). Therefore, highly sensitive methods are required for comprehensive identification and quantification of the TPs of benzothiazoles (Han and Zhang, 2018; Jiang et al., 2020).

Recent studies highlighted the ability of nontargeted analysis using high resolution mass spectrometry (HRMS) to obtain comprehensive information about the unknown TPs at trace levels in wastewater and drinking water (Fu et al., 2017; Liberatore et al., 2017; Tang et al., 2020; Tang et al., 2016). Herein, we report on the development of a novel nontargeted strategy using high performance liquid chromatography–high resolution mass spectrometry (HPLC–HRMS) to comprehensively identify molecular structures of the unknown products of 2-MBT in water upon UV treatment. The identified TPs were confirmed when standards were available. The mass balance of TPs was analysed over the UV degradation of 2-MBT. Based on the identified TPs and their patterns over the UV exposure times we postulated the mechanism of 2-MBT photodegradation. Lastly, we applied established computational assessment methods to evaluate potential aquatic toxicity and the effects of 2-MBT and its TPs on the enzyme/hormones regulating the thyroid function to identify the TPs of toxicological relevance. To the best of our knowledge, this is the first study reporting on mass

balance in combination with the computational toxicity estimates for unknown TPs and their isomers generated during UV photolysis of benzothiazoles in water. The outcomes of this study on 2-MBT photolysis raise the awareness on the need for a comprehensive approach to the examination of micropollutant treatment in water and on potential unintended consequences on the treated water quality.

2. Materials and methods

2.1. Chemicals and solutions

2-Mercaptobenzothiazole (2-MBT) (97%), benzothiazole (BT) (96%), 2-hydroxybenzothiazole (2-OH-BT) (98%), 2-benzothiazolesulfonic acid potassium salt (2-SO₃-BT), and 2-aminobenzaldehyde (≥98%) were obtained from Sigma-Aldrich (St. Louis, MO, USA). Benzo[d]thiazol-4-ol (4-OH-BT) (98%), benzo[d]thiazol-5-ol (5-OH-BT) (>95%), and 6-hydroxybenzothiazole (6-OH-BT) (>95%) were obtained from BLD Pharmatech (Shanghai, China). Potassium phosphate monobasic (KH₂PO₄) (99%), sodium hydroxide (NaOH) (99%), Optima LC/MS grade water, methanol (MeOH), acetonitrile (ACN), formic acid (FA, 98% in water) for mass spectrometry were purchased from Fisher Scientific (Ottawa, ON, Canada). Phosphoric acid (H₃PO₄) (85%) was obtained from Caledon Laboratories Ltd (Georgetown, ON, Canada).

The 2-MBT (10 mg/mL) stock solution was prepared in ACN every two weeks and kept in amber glass vials with minimum headspace to reduce/eliminate the slow oxidation of 2-MBT in the dark by the oxygen present at ambient conditions. Stock solutions for other BT derivatives and 2-aminobenzaldehyde (0.33–20 mg/mL) were prepared individually in ACN. All stock solutions were stored in amber glass vials in the refrigerator at 4°C. The stock solutions of KH₂PO₄ (50 mM), NaOH (100 mM), and H₃PO₄ (100 mM) were prepared separately in Optima water. Phosphate buffer (0.5 mM) was prepared by diluting the concentrated stock KH₂PO₄ solution and adjusting pH to the required value using NaOH or H₃PO₄ stock solutions.

2.2. UV experimental set-up

UV photolysis of 2-MBT was performed with a bench scale collimated beam device as shown in **Fig. S1**. Two-8W UVC germicidal lamps (LZC-UVC-01, Luzchem Research Inc., Ottawa, ON, Canada), emitting primarily at 253.7 nm, were mounted at the top center of the photoreactor (Luzchem-LZC-4V). The aperture diameter for the collimated UV light beam was 11.5 cm. Sample aliquots of 46 mL were transferred to a crystallizing dish (60 mm diameter × 35 mm depth) (VWR, Radnor, PA, USA) and exposed to the UV radiation for predetermined periods of time. The distance from the lamps to the solution surface was 17.9 cm and the sample depth was 2.1 cm. The UV irradiance at the surface of water was measured with a UVX model digital radiometer. During the irradiation, the water sample was stirred continuously. The average UV fluence was calculated according to the standardized method reported by Bolton and Linden (Bolton and Linden, 2003). Details on the UV fluence calculations are given in **Section S1** and **Table S1**. In this study, the target UV fluences were set at 500, 1000, 2000, 3000, 4000, 5000, and 6000 mJ/cm².

For the UV irradiation experiments, the 2-MBT (about 500 µg/L) working solution was prepared by adding 50 µL of 2-MBT stock solution (10 mg/mL in ACN) to 1-L volumetric flask with phosphate buffer (0.5 mM) at pH 7.6. The ACN content in the working solution was 0.005%. The working solution was protected from the ambient light with aluminum foil over the duration of the experiments. The UV absorbance of the working solution was measured

in triplicate within 1 h before irradiation to confirm the complete dissolution and stability of 2-MBT, and an average value was considered for UV fluence calculation. At the end of each exposure, a 10-mL aliquot of UV-irradiated 2-MBT solution was taken for immediate UV absorbance measurement. A 2-mL aliquot was taken for HPLC-MS analysis without pretreatment. The remaining irradiated solution was kept for inductively coupled plasma mass spectrometry (ICP-MS) and IC analysis. All aliquots were kept in amber glass vials without headspace.

2.3. Nontargeted HPLC-HRMS analysis

The analytes in the 2-MBT solutions before and after UV irradiation were separated on an Accucore C18 column (150 × 2.1 mm i.d., 2.6 μm; pore size, 80 Å; Thermo Scientific, Waltham, MA, USA) using an Agilent HPLC system (Agilent 1290 HPLC). A quadrupole time-of-flight (QTOF) high-resolution mass spectrometer (SCIEX X500R; SCIEX, Concord, ON, Canada) with a Turbo-V electrospray ionization (ESI) source was used in positive and negative modes to obtain accurate mass measurements of the $[M+H]^+$ or $[M-H]^-$ ions. The details of the HPLC-HRMS conditions were described in **Section S2**. Tandem mass (MS/MS) spectra were collected for each sample using information dependent acquisition (IDA) mode. The scan cycle of IDA contained two experiments. The first experiment was designed to run a full scan analysis and the second experiment was used to collect MS/MS spectra of 10 most intense molecular ions whose intensity exceeded a designated value (i.e., 1000 cps in this study). The IDA parameters were presented in **Section S3**.

Qualitative and quantitative data analysis was performed using SCIEX OS software. A nontargeted strategy was used for identification of 2-MBT and its degradation products. In detail, each solution before and after UV treatment for 1.5 min to 25 min was analyzed using nontargeted analysis of the HPLC-HRMS under predefined parameters. The acquired HPLC-HRMS data file contained the retention time, $[M+H]^+$ from positive ESI or $[M-H]^-$ from negative ESI, and peak intensity. By comparing the data from the sample (2-MBT solutions exposed to the UV radiation) to the control (2-MBT solutions kept in the dark), we identified peaks that were detected exclusively in the sample, but not in the control. A peak was considered as a newly formed product when its signal intensity in the sample was 10 times higher than the background. For the identification of the degradation products generated during the UV exposure of 2-MBT solutions, we acquired the accurate m/z ($[M+H]^+$ or $[M-H]^-$) and MS/MS spectra of the products using the IDA experiments. Commercial authentic standards when available were purchased for confirmation of the products. Additionally, the quantitation of the new compounds was performed using external calibration curves.

2.4. Analysis of inorganic anions

Ion chromatography (Dionex DX-600) was used to examine the generation of inorganic degradation products (i.e., NO_2^- , NO_3^- , and SO_4^{2-}) from UV irradiation of 2-MBT solutions. The work was done in the Biogeochemical Analytical Service Laboratory (BASL) at the University of Alberta using the US EPA Method 300.1. The total of NO_2^- and NO_3^- was measured using a Lachat QuickChem QC8500 flow injection analysis automated ion analyzer at BASL as described in the US EPA Method 353.2.

2.5. Computational assessment of aquatic toxicity and effects on thyroid enzyme function

The aquatic toxicity of 2-MBT and its TPs was assessed using the ecological structure activity relationships (ECOSAR) model

(USEPA, 2020). Herein, fish was selected as a target aquatic species due to the significance as food for many species including humans. The aquatic toxicity to fish is expressed as median lethal concentration (LC_{50}) after fish 96-h exposure. The lowest effect concentration was reported considering the conservative prediction for the precautionary principle. To assess potential human health effects, we examined effects of 2-MBT and its TPs on thyroid hormones using Danish QSAR database consisting of over 650,000 compounds (Danish(Q)SAR 2015; Rosenberg et al., 2016). Thyroperoxidase (TPO) is the key enzyme for synthesis of thyroid hormones, thus we focused on the inhibition effect of 2-MBT and TPs on TPO activity. The Danish QSAR model predicts probability (p) value between 0 and 1 for a test compound to inhibit TPO activity: as the p value close to 1, the ability of the test compound to inhibit TPO activity is higher.

In addition to the tests described above, the estrogenic activity of transformation products was evaluated using VirtualToxLab package (Vedani et al., 2015; Vedani et al., 2012; Vedani and Smiesko, 2009).

3. Results and discussion

3.1. Nontargeted identification of TPs: positive ESI

Initial UV spectrometry measurements of the samples before and after UV irradiation indicated the photodegradation of 2-MBT, supported by the appearance of a new product peak at ~217 nm and a significant change in the UV spectrum (**Fig. S2**). Total ion chromatographs recorded during HPLC-MS analysis only show the disappearance of 2-MBT but no information on byproducts (**Fig. S3**). The details are described in **Section S4-5** of Supplementary Information. In order to identify the 2-MBT transformation products and characterize their dynamics upon UV exposure, we have developed and applied a nontargeted comprehensive analytical approach. The nontargeted strategy involves acquisition of full scan MS data (m/z 50-500) of the treated and untreated samples, comparing the full scan data of the sample with the control to identify new products, and followed by a second run in IDA mode to acquire MS/MS spectra of the new products.

Through comparison of the MS data (m/z 50-500) of the treated samples with the control sample without UV irradiation, twelve unknown peaks were consistently detected in the UV treated samples using HPLC-QTOF-MS in positive ESI mode. **Fig. 1** shows the extracted ion chromatograms (EICs) of the unknowns (peaks P1-P12) discovered using the nontargeted strategy. Among the unknowns, peaks P2-P5 had the same m/z value of 152.0176 but eluted at different retention times, indicating that they are isomers. Similarly, peaks P8-P12 are isomers of m/z value of 168.0125. **Table 1** summarizes the m/z values, retention times, predicted molecular formulas, and the corresponding mass errors of the twelve TPs (peaks P1-12), as well as their confidence levels according to Schymanski scale (Schymanski et al., 2014). The determination of the accurate masses of the detected TPs enabled the prediction of their molecular formulas. The difference between the theoretical and measured molecular weights of the TPs was less than 10 ppm, supporting their tentative identification.

To further elucidate the structures of the detected 12 TPs (**Table 1** and **Fig. 1**), we used the method of HPLC-QTOF-MS in IDA mode. The IDA method acquired the accurate mass of precursor ions by TOF full scans followed by the MS/MS spectra of the product ions. P7 was detected as one of the major products. The protonated molecular ion of P7 (m/z 136.0226) predicted its molecular formula as $\text{C}_7\text{H}_5\text{NS}$ that matched with benzothiazole (BT). Next, P7 was confirmed by matching its retention time (**Fig. 1**), MS and MS/MS spectra with those of the benzothiazole standard (**Fig. 2**). Thus, P7 was confirmed as benzothiazole. Furthermore, P1 differed

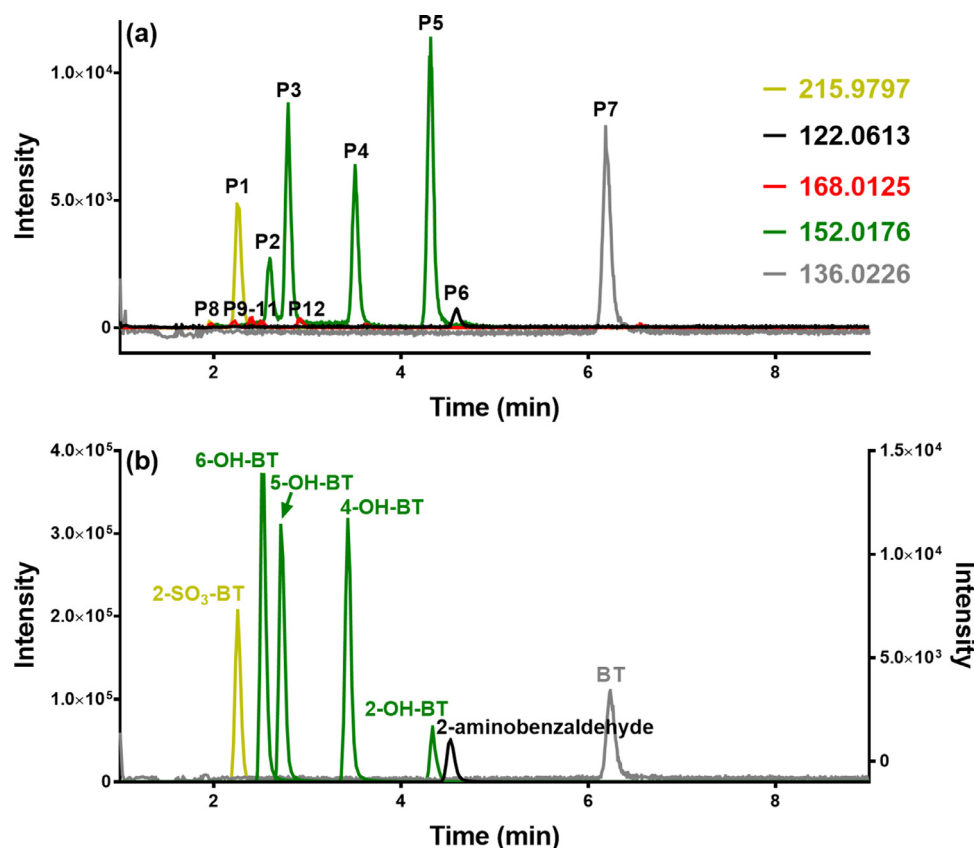


Fig. 1. (a) EICs of unknowns P1–P12 detected in the 2-MBT solution exposed to a UV fluence of 3000 mJ/cm² (b) EICs of BT standards. Note: 6-OH-BT, 5-OH-BT, and 4-OH-BT were plotted against the right y-axis.

Table 1
Unknowns detected by nontargeted analysis for 2-MBT treated with UV.

Unknowns	Mass/charge	ESI polarity	Retention time (min)	Predicted molecular formula	Mass error (ppm)	Confidential Level
P1	215.9797	Pos	2.28	[C ₇ H ₅ NO ₃ S ₂ + H] ⁺	6.0	Level 1
P2	152.0176	Pos	2.63	[C ₇ H ₅ NOS + H] ⁺	7.2	Level 1
P3	152.0176	Pos	2.83	[C ₇ H ₅ NOS + H] ⁺	7.2	Level 1
P4	152.0176	Pos	3.56	[C ₇ H ₅ NOS + H] ⁺	7.2	Level 1
P5	152.0176	Pos	4.38	[C ₇ H ₅ NOS + H] ⁺	7.2	Level 1
P6	122.0613	Pos	4.64	[C ₇ H ₇ NO + H] ⁺	10	Level 1
P7	136.0226	Pos	6.26	[C ₇ H ₅ NS + H] ⁺	8.1	Level 1
P8	168.0125	Pos	1.99	[C ₇ H ₅ NO ₂ S + H] ⁺	6.5	Level 3
P9	168.0125	Pos	2.23	[C ₇ H ₅ NO ₂ S + H] ⁺	6.5	Level 3
P10	168.0125	Pos	2.52	[C ₇ H ₅ NO ₂ S + H] ⁺	6.5	Level 3
P11	168.0125	Pos	2.96	[C ₇ H ₅ NO ₂ S + H] ⁺	6.5	Level 3
P12	168.0125	Pos	3.67	[C ₇ H ₅ NO ₂ S + H] ⁺	6.5	Level 3
P13	181.9916	Neg	1.93	[C ₇ H ₅ NO ₃ S - H] ⁻	0.6	Level 3
P14	245.9350	Neg	2.26	[C ₇ H ₅ NO ₃ S ₃ - H] ⁻	3.2	Level 3

from P7 with a unit of SO₃ as well as a fragment ion matched with [M-SO₃]⁺ (Fig. 2). After comparing the retention time and MS/MS spectrum of P1 with the standard BT-SO₃, we confirmed P1 as benzothiazole-2-sulfonic acid (2-SO₃-BT).

Peaks P2–P5 had a protonated molecular mass of 152.0176, which differed from benzothiazole (P7) by an oxygen atom, indicating an oxygen atom added to the benzothiazole structure. In the MS/MS spectra of P2–P5, a characteristic fragment ion of *m/z* 134.0056–134.0067 was detected, corresponding to the loss of the -OH group from the precursor molecule (i.e., [M-OH]⁺). This observation strongly suggested that P2–P5 were mono-hydroxylated benzothiazole isomers. To confirm the identity of each isomer, we compared P2–P5 with commercially available standards. As shown in Figs. 1–2, the retention times and MS/MS spectra of P2–P5 matched those of standards 6-OH-BT, 5-OH-BT, 4-OH-BT, and 2-

OH-BT, respectively. 2-OH-BT was confirmed with the standard 2-hydroxybenzothiazole. Additionally, the product 2-OH-BT can exist in two tautomeric forms as shown in Fig. S4. Similarly, P6 had a predicted molecular formula of C₇H₇NO (Table 1) without any S atoms. Upon examination of the MS/MS spectrum and comparison with the standards, P6 was confirmed as 2-aminobenzaldehyde (Section S6 and Figs. 1 and 2).

Low intensity peaks were also detected using the nontargeted strategy. For example, five peaks were detected with retention time values of 1.99, 2.23, 2.52, 2.96 and 3.67 min. Due to the low intensity of the MS signals, acquisition of the MS/MS spectra of these peaks was difficult. However, based on the one MS/MS spectrum collected (Fig. S5), we observed two equivalent mass losses (18.0121 and 17.9986), suggesting that this compound possibly contains two hydroxyl groups. The fragment 132.0041 also

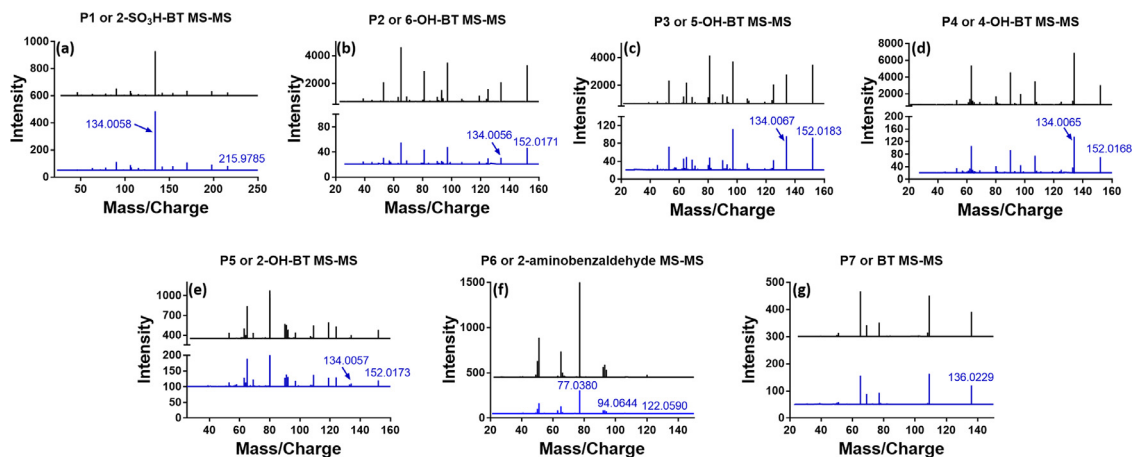


Fig. 2. MS/MS spectra collected from the 2-MBT solution after exposure to a UV fluence of 4000 mJ/cm² (blue) and commercially available BT standards (black). (For interpretation of the references to color in this figure legend, the reader is referred to the web version of this article.)

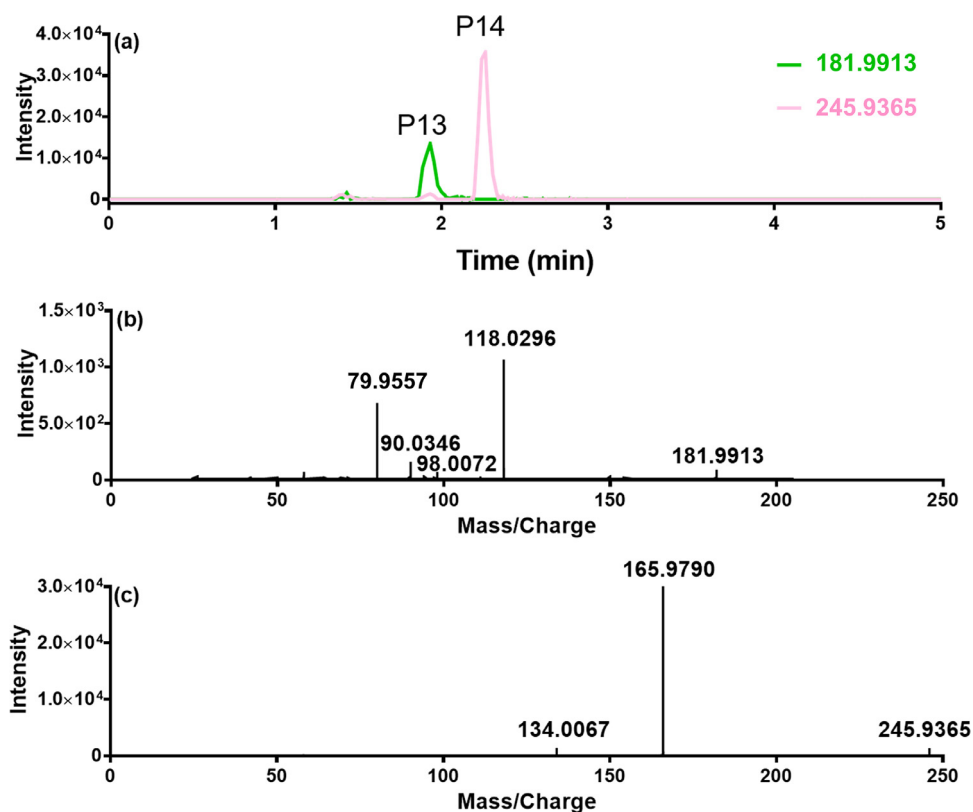


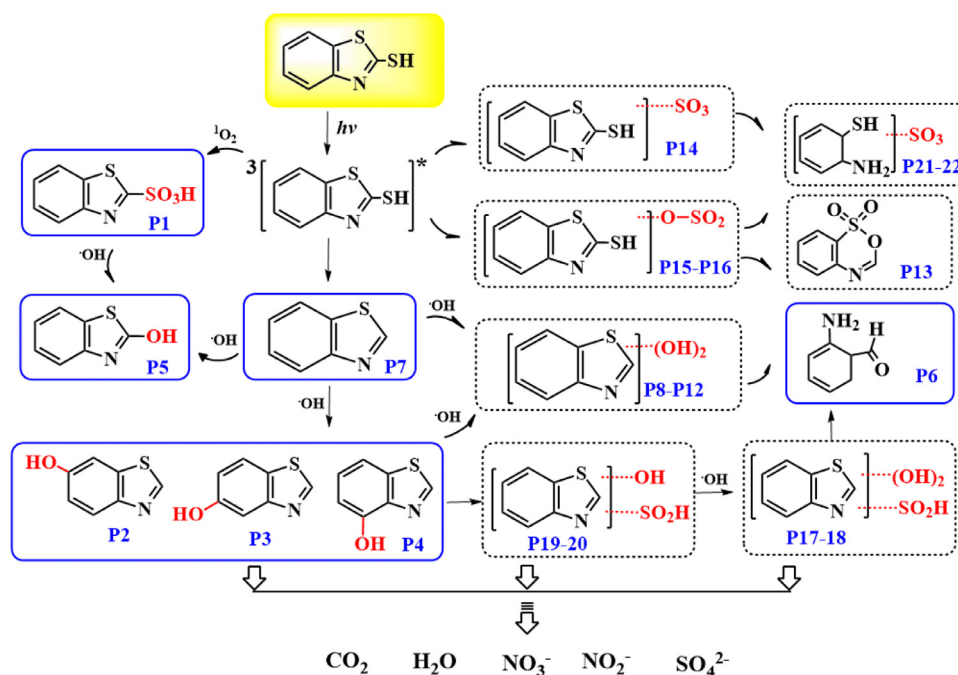
Fig. 3. (a) EICs of unknowns P13 and P14 detected in the 2-MBT solution exposed to a UV fluence of 3000 mJ/cm². MS/MS spectrum for (b) 181.9 at 1.9 min and (c) 245.9 at 2.3 min.

matched with [BT-2H]⁺, indicating that the parent molecule may contain the BT core structure. Thus, it is reasonable to tentatively identify P8–P12 as the isomers [BT-(OH)₂] of di-hydroxy-BTs and their tautomers. Because of the lack of authentic standards, the confirmation of these structures was not possible at this time.

3.2. Nontargeted identification of TPs: negative ESI

Using negative ESI, the nontargeted LC-HR-MS/MS strategy revealed two additional unknowns in the irradiated 500 μg/L 2-MBT solution (Table 1). Fig. 3a shows the EICs of the two unknowns P13 and P14. The intensity of these two peaks was too weak to identify their structures. To obtain better quality MS/MS spectra

(Fig. 3b–c) for the structure identification, we performed the UV irradiation of a 2 mg/L 2-MBT solution. The accurate mass of P13 (181.9913) predicted its molecular formula as C₇H₅NO₃S. The mass difference between its deprotonated molecular mass (181.9913) and fragment ion *m/z* 118.0296 is 63.9617, corresponding to the loss of an SO₂ (calculated mass: 63.9618) group. Additional loss of a CO (calculated mass: 27.9949) group and a C₇H₄N (calculated mass: 102.0344) fragment were observed from 118.0296 to 90.0346 (observed mass loss: 27.9950) and 181.9913 to 79.9567 (observed mass loss: 102.0346), respectively. Furthermore, a fragment of 79.9567 matched with SO₃ (calculated mass: 79.9573). Based on these MS/MS fragments and mass losses, we proposed two possible structures, namely, benzo[d]thiazol-2(3H)-one 1,1-dioxide (A) and 2-oxa-2H-1,4-benzothiazine 1,1-dioxide (B), as depicted in Fig.



Scheme 1. Proposed pathways of formation of the transformation products generated during the photodegradation of 2-MBT at UV 253.7 nm (Note: structures in blue solid line box (P1-P7) were confirmed using commercially available standards. Structures in in dotted line box (P8-P22) were putatively identified using accurate MS and MS/MS spectra.).

S6. The simulated MS/MS spectra of the proposed structures were obtained using the SCIEX OS software, which were further compared with the experimental spectrum of P13 (Fig. 3b). The simulated spectra of structures (A) and (B) matched that shown in Fig. 3b at 61.6% and 93.5%, indicating that P13 has a closer resemblance to structure (B), i.e. 2-oxa-2H-1,4-benzothiazine 1,1-dioxide.

Similarly, the accurate mass of P14 predicted its molecular formula of $C_7H_5NO_3S_3$ and its characteristic fragment ions of m/z 134.0067 and 165.9790 corresponded to BT and deprotonated MBT, respectively. The detection of MBT fragment of m/z 165.9790 indicated that an S atom was within the BT core structure. The mass difference between the parent ion of m/z 245.9365 and a fragment ion of m/z 165.9790 was 79.9575, corresponding to a neutral loss of SO_3 . Therefore, P14 was rationally identified as MBT- SO_3 .

The UV irradiation of 2-MBT at higher concentration (2 mg/L) enabled the detection of additional unknown products associated with peaks P15–P22 in Fig. S7. Under the original LC conditions, these new peaks overlapped, making their identities ambiguous. To clarify whether these peaks were degradation products or fragments of larger molecules produced in the ESI source, we modified the LC method to improve their separation. As shown in Figs. S8–S9, these peaks between the two red lines were resolved from each other under the optimized LC conditions of Fig. S9. This supports that these peaks resulted from UV degradation, not fragments in the ion source. Table S2 presents the accurate masses and the molecular formula of these TPs, including the eight compounds detected in Fig. S7. The MS/MS spectra (Figs. S10–S13) were also acquired for the peaks listed in Table S2. The two spectra in Figs. S10–S13 are very similar, indicating that these are structure isomers. For example, in Fig. S10a–b, the presence of fragments of 134.0057 ((a) and (b)) and 165.9789(a)/165.9815(b) suggested that both P15 and P16 had the $[M-H]^-$ of 245.9350 and molecular formula of $C_7H_5NS_3O_3$ and contained the 2-MBT structure. Meanwhile, the mass difference between the fragment ion 181.9 and the parent ion 245.9 matched with the loss of an SO_2 unit. The mass difference between the fragment ion 165.9 and parent ion 245.9 matched with the loss of an SO_3 unit. Therefore, the P15 and

P16 were rationally identified as 2-MBT derivatives with a $-O-SO_2H$ group.

P17 and P18 had similar MS/MS spectra suggesting them as isomers, as shown in Fig. S11 a and b. For instance, the mass difference between m/z 229.9620 and m/z 165.9973 matched with the loss of an SO_2 unit, while the mass difference between m/z 229.9620 and 201.9664 corresponded to the loss of $-CO$. In addition, the fragment ions of m/z 150.0031/150.0045 matched with the deprotonated hydroxylated BT. Thus, P17 and P18 were identified as BT derivatives substituted with two $-OH$ groups and one $-SO_2$ group. Similarly, the MS/MS spectra of P19 and P20 (Fig. S12a–b) suggested them as BT derivatives substituted with one $-OH$ group and one $-SO_2$ group.

The accurate masses of the unknowns P21 and P22 predicted their molecular formula of $C_6H_7NS_2O_3$, indicating the opening of the BT core structure. The mass shift from 203.9790 to 171.0019 was 32.9771, in agreement with the loss of an $-SH$ group. The mass shift from 203.9790 to 124.0234 is 79.9556, matched with the loss of an $-SO_3$ unit. These suggested that P21 and P22 resulted from the opening of a thiazole ring and with the loss of a carbon, i.e., the 2-aminothiophenol structure. P21 and P22 were identified as 2-aminothiophenol- SO_3 . The accurate mass and MS/MS spectra of the unknowns P15–22 suggested their structures as shown in Scheme 1.

In short, the nontargeted HPLC-HRMS approach enabled the identification of the nine new products (P2–P4, P13–P16, P21–P22) for the first time, adding new information about the photodegradation of 2-MBT to previously reported products including benzothiazole-2-sulfonate (P1), 2-hydroxybenzothiazole (P5), benzothiazole (P7) in wastewater effluents and surface water (Summarized in Table S3) (Li et al., 2006; Malouki et al., 2004; Serdechnova et al., 2014; Zajíčková and Párkányi, 2008; 2009). The occurrence of these products (P1, P5, P7) was also reported during the biological treatment of wastewater in Germany (Kloepfer et al., 2004). Reemtsma (2000) showed that the concentrations of P1 and P5 in the wastewater effluent were 2.6 and 20 times higher than their concentrations at the plant intake, respectively, indicating

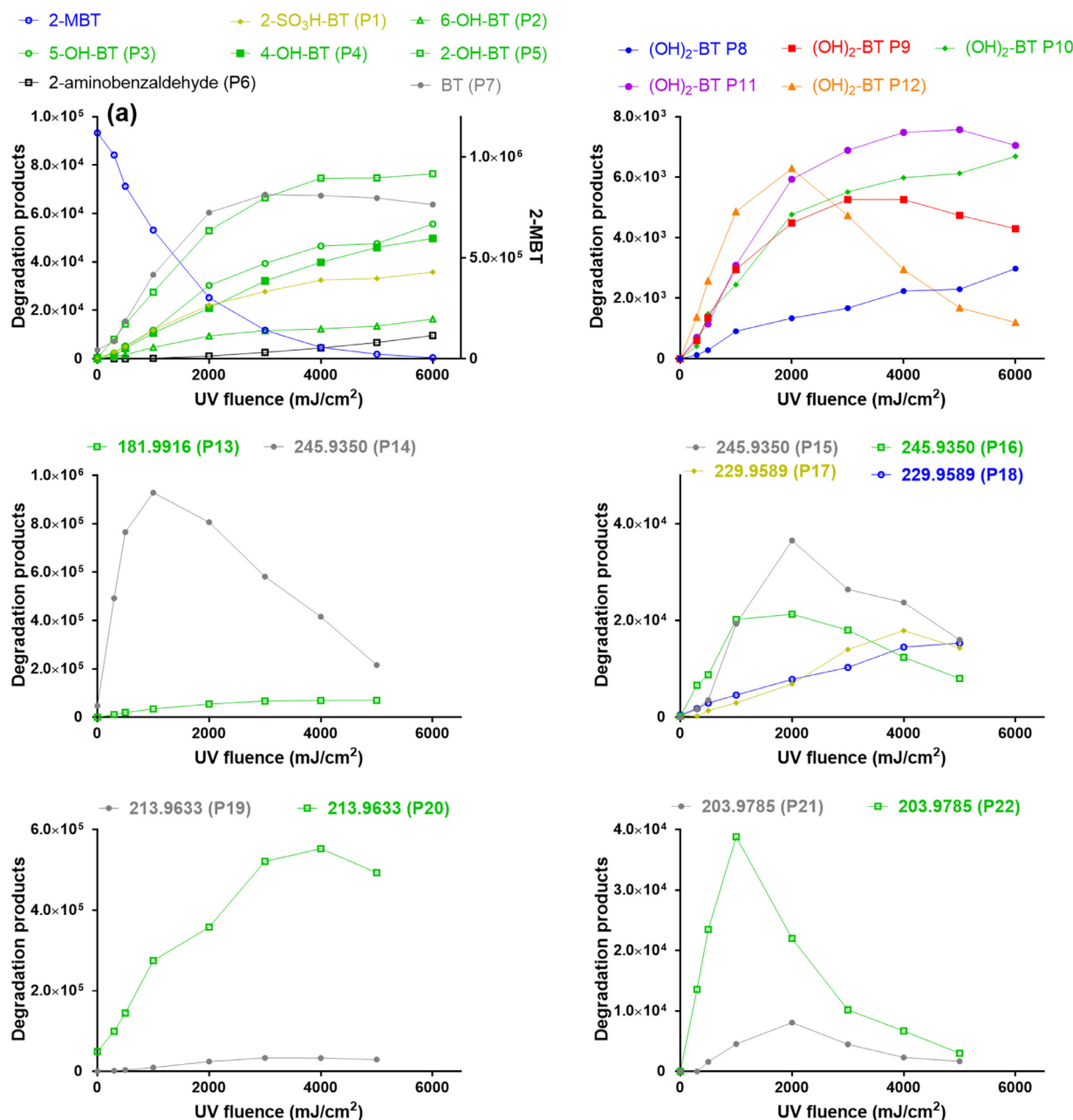


Fig. 4. Change of intensity of 2-MBT and its UV transformation products (P1–P22) with UV fluence.

the formation of these products during the treatment processes. Particularly, identification of isomeric new products (P2–P4) of 2-hydroxybenzothiazole (P5) demonstrates the capability of the new nontargeted HPLC–HRMS strategy developed and implemented in this study. These new TPs were further evaluated for their toxicological relevance as described in Section 3.5.

3.3. Quantification of organic and inorganic TPs

Fig. 4 shows the intensities of the major and minor UV degradation products of 2-MBT in a solution of pH 7.6 with varying UV fluence. As the UV fluence increases from 500 to 6000 mJ/cm², 2-MBT decreased rapidly. The majority of the TPs increased with the increasing UV fluence, whereas five of the TPs (P12 and P14–16) first increased and then decreased, indicating that they are susceptible to UV photolysis. On the contrary, the majority of formed TPs (e.g. P1, P2, P4, P5, P8, P10, P18) appear to accumulate in the solu-

tion, which indicates that they are relatively resistant to UV degradation as compared to the original 2-MBT. 2-Aminobenzaldehyde (P6) was not detected until the UV fluence reached 1000–2000 mJ/cm². This suggested that 2-aminobenzaldehyde was likely a secondary product.

Using the available standards and external calibration curves, we quantified 2-MBT and the major degradation products generated during the UV (253.7 nm) irradiation of 2-MBT solutions. The results are summarized in Fig. S14. Because all the major transformation products (Scheme 1 P1–5 and P7) contained the BT core structure, we rationally proposed that one 2-MBT molecule produced one molecule of the degradation product. Fig. S15 shows the molar fraction of remaining 2-MBT and each degradation product as a function of UV fluence. At an UV fluence of 3000 mJ/cm², approximately 13% of 2-MBT remained while the sum of the major degradation products accounted for approximately 57% of the original 2-MBT. In total, approximately 70% of the original 2-MBT

can be tracked using our LC-MS method while 30% is missing. At an UV fluence of 6000 mJ/cm², the missing mass balance increased to 40% (**Table S4**). The missing balance could be represented by the TPs that were not quantified due to the lack of commercially available standards. Alternatively, 2-MBT could have been partly mineralized to inorganic products. At a UV fluence of ~40 mJ/cm² which is typically employed for drinking water disinfection, no noticeable degradation of 2-MBT was observed (Fig. S15). At a UV fluence of ~1000 mJ/cm² which would degrade ~90% of N-nitrosodimethylamine (NDMA) in potable reuse applications, approximately 50% 2-MBT was photolyzed to the major product BT along with minor products 2-SO₃-BT and 2-OH-BT (Fig. S16). Of note, both 2-MBT and its byproducts are very efficiently treated via hydroxyl radical-initiated oxidations in the UV/H₂O₂ AOP (Bahnmüller et al., 2015; Andreozzi et al., 2001), which is largely practiced at drinking water and potable reuse water treatment plants around the world.

To investigate the inorganic degradation products, we carried out ICP analysis of the total sulfur (S) content in the 2-MBT solutions before and after UV treatment without pretreatment of the samples (**Fig. S17**). The S content in the irradiated sample did not change significantly compared to the initial 2-MBT solution, indicating that all the sulfur from 2-MBT remained in the sample after UV radiation. Furthermore, to track the missing sulfur content, we hypothesized that other S-containing organic compounds or S-containing inorganic ions such as SO₄²⁻ are also formed. IC experiments provided a limit of detection of 0.04 mg/L for SO₄²⁻ and 6 µg/L for N in NO₂⁻+NO₃⁻. **Figure S18** shows that increasing UV fluence for treatment of 2-MBT increased the concentrations of SO₄²⁻ and NO₂⁻+NO₃⁻ formed. The formation of SO₄²⁻ likely resulted from the oxidation of the thiol group of 2-MBT. Additionally, the opening of the thiazole ring to form 2-aminobenzaldehyde involved the loss of S, which can lead to the formation of SO₄²⁻. The formation of SO₄²⁻ has also been observed from the gamma radiation process of 2-MBT (Bao et al., 2016). It is unclear how photodegradation of 2-MBT led to the formation of NO₂⁻+NO₃⁻, but it may have resulted from the oxidation of the thiazole ring of 2-MBT and/or the TPs containing the N atom.

3.4. Proposed UV degradation pathways of 2-MBT

Based on the structures of the identified TPs and mass balance results, the degradation pathways of 2-MBT with the UV (253.7 nm) radiation is tentatively proposed as shown in **Scheme 1**. The excited singlet state of 2-MBT (¹MBT*) is initially formed upon the absorption of UV radiation by 2-MBT. The excited singlet state likely deactivates rapidly to the longer-lived excited triplet state (³MBT*) (Koyama and Orr-Ewing, 2016). The main product P7 could be formed via C-SH bond cleavage, further resulting in the formation of hydroxylated products P2-P5, P8-P12. The photooxidation of -SH group could be the route to the sulfonic products P1, P14-P16, which in turn are the precursors of products P17-P20. Thiazole ring opening likely occurring at higher UV energies delivered to the samples would explain the formation of the observed products P6, P13, P21-P22, as well as of the inorganic ions.

The extensive investigation of pH effect on 2-MBT photolysis and on byproduct formation and characterization was beyond the scope of this work. Only two tests were performed at pH 3 and pH 10 for the purpose of observing the pH impact on 2-MBT degradation and major primary byproduct profiles. The trends are shown in Fig. S19. At pH 3, a minimal degradation of 2-MBT was observed over the entire UV fluence range. This observation is consistent with the low quantum yield ($\Phi < 0.01$) and small molar absorption coefficient ($\epsilon \sim 550$ m²/mol) of 2-MBT at 254 nm at pH 3 as compared to the values of these photochemical parameters at pH ~8-10 ($\Phi \sim 0.025$; $\epsilon \sim 800$ m²/mol) (Bahnmüller et al., 2015). The

major primary byproducts were identical at the three pH values tested, with BT, 2-OH-BT and 2-SO₃-BT concentrations increasing with the pH increase.

3.5. Computational toxicity assessment of 2-MBT and its organic TPs

To evaluate toxicological relevance of the twenty-two TPs of 2-MBT, we conducted computational quantitative structure-activity relationship (QSAR) analysis using the established models, including ECOSAR, Danish QSAR database, and VirtualToxLab package, as previously described (Danish(Q)SAR 2015; Gao et al., 2015; Gao et al., 2014; Rosenberg et al., 2016; USEPA, 2020). These QSAR predictive results, as shown in **Table S5**, **Figs. S20-22** and **Section S7**, include fish (LC₅₀) indicating aquatic toxicity and inhibition of thyroperoxidase (TPO) indicating potential effects on human health. The aquatic toxicity of the TPs is lower than that of 2-MBT. Interestingly, the TPs are predicted to increase inhibition of TPO activity compared to 2-MBT.

The LC₅₀ value of original 2-MBT to fish was predicted to be 1.57 mg L⁻¹. According to the toxicity criteria by European Union (Directive 67/548/EEC), 2-MBT is classified as Toxic Level (1.0 < LC₅₀ < 10.0 mg L⁻¹). Four TPs (P5 and P8-P10) were predicted to have LC₅₀ (3.79 - 9.48 mg L⁻¹), slightly higher than 2-MBT (**Fig. S20**), but within the Toxic Level defined by EUC. Similarly, other seven TPs (P2-P4, P6-P7, P11-P12) were classed as harmful to fish (10.0 < LC₅₀ < 100.0 mg L⁻¹), and the remaining TPs were non-harmful (LC₅₀ > 100.0 mg L⁻¹). Thus, the adverse effects of four products (P5 and P8-P10) on aquatic organisms should not be ignored, although their aquatic toxicity decreased with the UV degradation of 2-MBT.

2-MBT has been reported to disrupt thyroid hormones by inhibiting thyroxine release. TPO is the enzyme that synthesizes thyroid hormones. Computational predictions of TPs as compared to 2-MBT are shown in **Fig. S21**. Herein, the probability (p) (Rosenberg et al., 2017), between 0 and 1 was predicted for a tested compound to inhibit the key enzyme TPO. Except for four TPs (P1, P5, P7, P13), the remaining 18 TPs could increase the probability of inhibition activity of TPO. In particular, most TPs (P2, P3, P4, P6, P9-P12, P15-P22) show distinct probability for disrupting thyroid hormones with the probability values greater than 0.70. Of course, *in vitro/in vivo* experimental research is necessary to further confirm the accurate toxicity value of these TPs. Additionally, the four hydroxylated products P2-P5 are isomers and confirmed by commercially available standards. Other studies have observed hydroxylated products of micropollutants that show increased estrogenic effects due to potential interaction of their hydroxyl group with estrogen receptor (Cao et al., 2018; Mboula et al., 2015). Thus, the estrogenic activity of these products were analyzed (Section S7), showing the higher estrogenic activity of the three isomers (P2-4) than P5. These predictive results indicate the toxicological importance of the TPs. Therefore, simple reducing concentration and aquatic toxicity of 2-MBT is not sufficient to reduce potential adverse effects on human health.

4. Conclusions

This study demonstrates the ability of the developed nontargeted analysis method to identify accurately the structures of 9 new and 13 known organic TPs resulting from UV treatment of water containing 2-MBT. The molar-based mass balance study accounted for 70% of the organic TPs and 30% of inorganic products. The comprehensive chemical structure information acquired on the identified products and their UV fluence-based dynamic patterns suggested potential multiple pathways of UV degradation of 2-MBT in water via photo-induced bond cleavage, hydroxylation, and oxidation. In addition, the structure identification of the new TPs en-

abled QSAR predictions on their potential toxicity on aquatic organisms and human health, whereas the predicted higher estrogenic activity of the identified isomeric TPs (P2-P4) than that of 2-hydroxybenzothiazole (P5), a well-known toxic contaminant, indicated the potential toxicological relevance of the new TPs.

Declaration of Competing Interest

The authors declare that they have no known competing financial interests or personal relationships that could have appeared to influence the work reported in this paper.

Acknowledgments

This study was supported by grants from Alberta Innovates, Alberta Health, the Natural Sciences and Engineering Research Council (NSERC) of Canada, and Canada Research Chairs, as well as National Natural Science Foundation of China (41977365). PJ acknowledges the support of MITACS and Trojan Technologies for her postdoctoral fellowship. YG acknowledges the support of Guangdong University of Technology for her visiting scholarship.

Supplementary materials

Supplementary material associated with this article can be found, in the online version, at doi:10.1016/j.watres.2020.116542.

References

- Alsbaiee, A., Smith, B.J., Xiao, L.L., Ling, Y.H., Helbling, D.E., Dichtel, W.R., 2016. Rapid removal of organic micropollutants from water by a porous beta-cyclodextrin polymer. *Nature* 529, 190–194.
- Andreozzi, R., Caprio, V., Marotta, R., 2001. Oxidation of benzothiazole, 2-mercaptobenzothiazole and 2-hydroxybenzothiazole in aqueous solution by means of H₂O₂/UV or photoassisted Fenton systems. *J. Chem. Technol. Biotechnol.* 76 (2), 196–202.
- Avagyan, R., Sadiqsis, I., Bergvall, C., Westerholm, R., 2014. Tire tread wear particles in ambient air—a previously unknown source of human exposure to the biocide 2-mercaptobenzothiazole. *Environ. Sci. Pollut. Res.* 21 (19), 11580–11586.
- Bahn Müller, S., Loi, C.H., Linge, K.L., von Gunten, U., Canonica, S., 2015. Degradation rates of benzothiazoles and benzothiazoles under UV-C irradiation and the advanced oxidation process UV/H₂O₂. *Water Res.* 74, 143–154.
- Bao, Q., Chen, L., Tian, J., Wang, J., 2016. Gamma irradiation of 2-mercaptobenzothiazole aqueous solution in the presence of persulfate. *J. Environ. Sci.* 46, 252–258.
- Bolton, J.R., Linden, K.G., 2003. Standardization of methods for fluence (UV dose) determination in bench-scale UV experiments. *J. Environ. Eng.* 129 (3), 209–215.
- Bond, T., Chu, W., von Gunten, U., Farré, M.J., 2020. Themed issue on drinking water oxidation and disinfection processes. *Environ. Sci.* 6, 2252–2256.
- Brownlee, B.G., Carey, J.H., Macinnis, G.A., Pellizzari, I.T., 1992. Aquatic environmental chemistry of 2-(thiocyanomethylthio) benzothiazole and related benzothiazoles. *Environ. Toxicol. Chem.* 11 (8), 1153–1168.
- Cao, H., Li, X., Zhang, W., Wang, L., Pan, Y., Zhou, Z., Chen, M., Zhang, A., Liang, Y., Song, M., 2018. Anti-estrogenic activity of tris(2,3-dibromopropyl) isocyanurate through disruption of co-activator recruitment: experimental and computational studies. *Arch. Toxicol.* 92 (4), 1471–1482.
- Danish(Q)SAR (2015), <http://qsar.food.dtu.dk/> (accessed October 14, 2020).
- Esmaili, N., Mofavvaz, S., Shabaneh, S., Sohrabi, M.R., Torabi, B., 2020. A simple colorimetric method using gold nanoparticles for the detection of 2-mercaptobenzothiazole in aqueous solutions, soil and rubber. *Int. J. Environ. Anal. Chem.* doi:10.1080/03067319.2020.1779241, 12.
- European Union (EU), 2008. European Union risk assessment report N-Cyclohexylbenzothiazol-2-sulphenamide CAS 95-33-0; Office for Official Publications of the European Communities <https://echa.europa.eu/documents/10162/52baf757-f74c-4993-84c8-3bb72195cf55>.
- Fiehn, O., Wegener, G., Jochimsen, J., Jekel, M., 1998. Analysis of the ozonation of 2-mercaptobenzothiazole in water and tannery wastewater using sum parameters, liquid- and gas chromatography and capillary electrophoresis. *Water Res.* 32 (4), 1075–1084.
- Fries, E., 2011. Determination of benzothiazole in untreated wastewater using polar-phase stir bar sorptive extraction and gas chromatography-mass spectrometry. *Anal. Chim. Acta* 689 (1), 65–68.
- Fu, Y.Q., Zhao, C.X., Lu, X., Xu, G.W., 2017. Nontargeted screening of chemical contaminants and illegal additives in food based on liquid chromatography-high resolution mass spectrometry. *Trends Anal. Chem.* 96, 89–98.
- Gao, Y., An, T., Ji, Y., Li, G., Zhao, C., 2015. Eco-toxicity and human estrogenic exposure risks from OH-initiated photochemical transformation of four phthalates in water: a computational study. *Environ. Pollut.* 206, 510–517.
- Gao, Y., Ji, Y., Li, G., An, T., 2014. Mechanism, kinetics and toxicity assessment of OH-initiated transformation of triclosan in aquatic environments. *Water Res.* 49, 360–370.
- Habibi, M.H., Tangestaninejad, S., Yadollahi, B., 2001. Photocatalytic mineralisation of mercaptans as environmental pollutants in aquatic system using TiO₂ suspension. *Appl. Catal. B* 33 (1), 57–63.
- Han, J., Zhang, X., 2018. Evaluating the comparative toxicity of dbp mixtures from different disinfection scenarios: a new approach by combining freeze-drying or rotoevaporation with a marine polychaete bioassay. *Environ. Sci. Technol.* 52 (18), 10552–10561.
- He, G., Zhao, B., Denison, M.S., 2011. Identification of benzothiazole derivatives and polycyclic aromatic hydrocarbons as aryl hydrocarbon receptor agonists present in tire extracts. *Environ. Toxicol. Chem.* 30 (8), 1915–1925.
- Jiang, J., Han, J., Zhang, X., 2020. Nonhalogenated aromatic DBPs in drinking water chlorination: a gap between NOM and halogenated aromatic DBPs. *Environ. Sci. Technol.* 54 (3), 1646–1656.
- Kloepfer, A., Gnirss, R., Jekel, M., Reemtsma, T., 2004. Occurrence of benzothiazoles in municipal wastewater and their fate in biological treatment. *Water Sci. Technol.* 50 (5), 203–208.
- Koyama, D., Orr-Ewing, A.J., 2016. Triplet state formation and quenching dynamics of 2-mercaptobenzothiazole in solution. *Phys. Chem. Chem. Phys.* 18 (37), 26224–26235.
- Lau, S.S., Wei, X., Bokenkamp, K., Wagner, E.D., Plewa, M.J., Mitch, W.A., 2020. Assessing additivity of cytotoxicity associated with disinfection byproducts in potable reuse and conventional drinking waters. *Environ. Sci. Technol.* 54 (9), 5729–5736.
- Li, F.B., Li, X.Z., Ng, K.H., 2006. Photocatalytic degradation of an odorous pollutant: 2-mercaptobenzothiazole in aqueous suspension using Nd³⁺-TiO₂ catalysts. *Ind. Eng. Chem. Res.* 45 (1), 1–7.
- Liao, C., Kim, U.-J., Kannan, K., 2018. A review of environmental occurrence, fate, exposure, and toxicity of benzothiazoles. *Environ. Sci. Technol.* 52 (9), 5007–5026.
- Liberatore, H.K., Plewa, M.J., Wagner, E.D., VanBriesen, J.M., Burnett, D.B., Cizmas, L.H., Richardson, S.D., 2017. Identification and comparative mammalian cell cytotoxicity of new iodo-phenolic disinfection byproducts in chloraminated oil and gas wastewaters. *Environ. Sci. Technol. Lett.* 4 (11), 475–480.
- Luongo, G., Avagyan, R., Hongyu, R., Östman, C., 2016. The washout effect during laundry on benzothiazole, benzotriazole, quinoline, and their derivatives in clothing textiles. *Environ. Sci. Pollut. Res.* 23 (3), 2537–2548.
- Rodríguez, D.M., Wrobel, K., Jiménez, M.G.G., Wrobel, K., 2004. Determination of 2-mercaptobenzothiazole (MBT) in wastewater by high performance liquid chromatography with amperometric detection. *Bull. Environ. Contam. Toxicol.* 73 (5), 818–824.
- Malouki, M.A., Richard, C., Zertal, A., 2004. Photolysis of 2-mercaptobenzothiazole in aqueous medium: laboratory and field experiments. *J. Photochem. Photobiol. A* 167 (2), 121–126.
- Margenat, A., Matamoros, V., Díez, S., Cañameras, N., Comas, J., Bayona, J.M., 2018. Occurrence and bioaccumulation of chemical contaminants in lettuce grown in peri-urban horticulture. *Sci. Total Environ.* 637–638, 1166–1174.
- Mboula, V.M., Héquet, V., Andrès, Y., Gru, Y., Colin, R., Doña-Rodríguez, J.M., Pastana-Martínez, L.M., Silva, A.M.T., Leleu, M., Tindall, A.J., Mateos, S., Falaras, P., 2015. Photocatalytic degradation of estradiol under simulated solar light and assessment of estrogenic activity. *Appl. Catal. B* 162, 437–444.
- Merle, T., Knappe, D.R.U., Pronk, W., Vogler, B., Hollender, J., von Gunten, U., 2020. Assessment of the breakthrough of micropollutants in full-scale granular activated carbon adsorbers by rapid small-scale column tests and a novel pilot-scale sampling approach. *Environ. Sci.* doi:10.1039/D0EW00405G.
- Mestankova, H., Parker, A.M., Bramaz, N., Canonica, S., Schirmer, K., von Gunten, U., Linden, K.G., 2016. Transformation of contaminant candidate list (CCL3) compounds during ozonation and advanced oxidation processes in drinking water: Assessment of biological effects. *Water Res.* 93, 110–120.
- Ni, H.-G., Lu, F.-H., Luo, X.-L., Tian, H.-Y., Zeng, E.Y., 2008. Occurrence, phase distribution, and mass loadings of benzothiazoles in riverine runoff of the Pearl River Delta, China. *Environ. Sci. Technol.* 42 (6), 1892–1897.
- Reddy, C.M., Quinn, J.G., 1997. Environmental chemistry of benzothiazoles derived from rubber. *Environ. Sci. Technol.* 31 (10), 2847–2853.
- Redouane-Salah, Z., Malouki, M.A., Khenouaoui, B., Santaballa, J.A., Canle, M., 2018. Simulated sunlight photodegradation of 2-mercaptobenzothiazole by heterogeneous photo-Fenton using a natural clay powder. *J. Environ. Chem. Eng.* 6 (2), 1783–1793.
- Reemtsma, T., 2000. Determination of 2-substituted benzothiazoles of industrial use from water by liquid chromatography/electrospray ionization tandem mass spectrometry. *Rapid Commun. Mass Spectrom.* 14 (17), 1612–1618.
- Richardson, S.D., Kimura, S.Y., 2017. Emerging environmental contaminants: challenges facing our next generation and potential engineering solutions. *Environ. Technol. Innovat.* 8, 40–56.
- Rosenberg, S.A., Nikolov, N.G., Dybdahl, M., Simmons, S., Crofton, K.M., Watt, E.D., Friedmann, K.P., Judson, R., Wedebye, E.B., 2016. Development of a QSAR Model for thyroperoxidase inhibition and screening of 72,526 REACH substances. *Toxicol. Lett.* 258, S116–S117.
- Rosenberg, S.A., Watt, E.D., Judson, R.S., Simmons, S.O., Paul Friedman, K., Dybdahl, M., Nikolov, N.G., Wedebye, E.B., 2017. QSAR models for thyroperoxidase inhibition and screening of U.S. and EU chemical inventories. *Comput. Toxicol.* 4, 11–21.
- Schymanski, E.L., Jeon, J., Gulde, R., Fenner, K., Ruff, M., Singer, H.P., Hollender, J., 2014. Identifying small molecules via high resolution mass spectrometry: communicating confidence. *Environ. Sci. Technol.* 48 (4), 2097–2098.

- Seeland, A., Oetken, M., Kiss, A., Fries, E., Oehlmann, J., 2012. Acute and chronic toxicity of benzotriazoles to aquatic organisms. *Environ. Sci. Pollut. Res.* 19 (5), 1781–1790.
- Serdechnova, M., Ivanov, L.V.M., Domingues, M.R., Evtuguin, V.D., Ferreira, G.S.M., Zheludkevich, L.M., 2014. Photodegradation of 2-mercaptobenzothiazole and 1,2,3-benzotriazole corrosion inhibitors in aqueous solutions and organic solvents. *Phys. Chem. Chem. Phys.* 16, 9.
- Sorahan, T., 2009. Cancer risks in chemical production workers exposed to 2-mercaptobenzothiazole. *Occup. Environ. Med.* 66 (4), 269–273.
- , 2018. Advanced oxidation processes for water treatment. In: Stefan, M.I. (Ed.), *Fundamentals and Applications*. IWA Publishing, London, UK.
- Tang, Y.N., Craven, C.B., Wawryk, N.J.P., Qiu, J.L., Li, F., Li, X.F., 2020. Advances in mass spectrometry-based omics analysis of trace organics in water. *Trends Anal. Chem.* 128, 115918. <https://doi.org/10.1016/j.trac.2020.115918>.
- Tang, Y.N., Xu, Y., Li, F., Jmaiff, L., Hrudey, S.E., Li, X.F., 2016. Nontargeted identification of peptides and disinfection byproducts in water. *J. Environ. Sci.* 42, 259–266.
- USEPA (2016) Provisional peer-reviewed toxicity values for 2-Mercaptobenzothiazole (CASRN 149-30-4), <https://cfpub.epa.gov/ncea/pprtv/documents/Mercaptobenzothiazole2.pdf>. (accessed October 14, 2020)
- USEPA, 2020. ECOSAR. United States Environmental Protection Agency <https://www.epa.gov/tsc-screening-tools/ecological-structure-activity-relationships-ecosar-predictive-model>.
- Vedani, A., Dobler, M., Hu, Z.Q., Smiesko, M., 2015. OpenVirtualToxLab-A platform for generating and exchanging in silico toxicity data. *Toxicol. Lett.* 232 (2), 519–532.
- Vedani, A., Dobler, M., Smiesko, M., 2012. VirtualToxLab - a platform for estimating the toxic potential of drugs, chemicals and natural products. *Toxicol. Appl. Pharmacol.* 261 (2), 142–153.
- Vedani, A., Smiesko, M., 2009. In silico toxicology in drug discovery - concepts based on three-dimensional models. *Atla-altern. lab. anim.* 37 (5), 477–496.
- Wang, L., Zhang, J.J., Sun, H.W., Zhou, Q.X., 2016. Widespread occurrence of benzotriazoles and benzothiazoles in tap water: influencing factors and contribution to human exposure. *Environ. Sci. Technol.* 50 (5), 2709–2717.
- Zajíčková, Z., Párkányi, C., 2008. Photodegradation of 2-mercaptobenzothiazole disulfide and related benzothiazoles. *J. Heterocyclic Chem.* 45 (2), 303–306.
- Zajíčková, Z., Párkányi, C., 2009. Monitoring of photodegradation process of various benzothiazoles by hplc and UV spectrometry: application of LC-MS in photo-product identification. *J. Liq. Chromatogr. Relat. Technol.* 32 (7), 1032–1043.